PROCEEDINGS OF SCIENCE

High energy gamma-ray emission detected by LHAASO from SNR G150.3+4.5

Houdun Zeng,[a,*] **Yingying Guo,**[a] **Hanrong Wu,**[b] **Yang Su,**[a] **Siming Liu**[c] **and Yi Zhang**[a] **for the LHAASO collaboration**

[a] *Key Laboratory of Dark Matter and Space Astronomy & Key Laboratory of Radio Astronomy, Purple Mountain Observatory, Chinese Academy of Sciences, 210023 Nanjing, Jiangsu, China*

[b] *Key Laboratory of Particle Astrophyics, Institute of High Energy Physics, Chinese Academy of Sciences, 100049 Beijing, China*

[c] *School of Physical Science and Technology, Southwest Jiaotong University, 610031 Chengdu, Sichuan, China*

E-mail: zhd@pmo.ac.cn

Recent observations and theories suggest that GeV cosmic-rays are dominated by SNRs interacting with molecular clouds while TeV cosmic-ray may have significant contributions from other sources, such as PWNes. Now LHAASO-WCDA have enough significance with E=1 TeV for SNR G150.3+4.5. Its spatial distribution and extension are consistent with that of the radio and the GeV band revealed by Fermi , and the extension of about 1.5 degrees. A source inside SNR G150.3+4.5 is detected by LHAASO-KM2A with a total significance of 9.4 sigma for E > 25 TeV. The best-fit source location is (R.A., Dec.)= $(66.63^\circ \pm 0.11^\circ, 54.63^\circ \pm 0.05^\circ)$, and the Gaussian extension is $0.32^\circ \pm 0.06^\circ$. It is spatially coincident with 4FGL J0426.5+5434, which has a soft GeV spectrum reminiscent of a pulsar. The broadband nonthermal emission can be interpreted as a contribution of a supernova remnant and a PWNe or high density molecular clouds interacting with high energy proton.

38th International Cosmic Ray Conference (ICRC2023)
26 July - 3 August, 2023
Nagoya, Japan

*Speaker

PoS(ICRC2023)606

1. INTRODUCTION

Supernova remnants(SNRs) have been considered as the main sites of Galactic cosmic-ray acceleration [1]. Charged particles are accelerated to relativistic energy through the diffusive shock acceleration(DSA) in the blast wave of supernova explosions [2]. The observation of several SNRs at GeV energies with the Fermi Large Area Telescope appear to the characteristic of the decay of neutral pion, resulting in the direct evidence that cosmic-rays are accelerated in SNRs [e.g. 3–6]. Although there is some potential evidence to support that some particles can reach PeV energies within SNRs [e.g. 7, 8], at the high-energy end, direct evidence of CR nuclei acceleration is still obscure. The maximum energy of γ-rays from SNRs can typically reach several tens of TeV [9] implying an ion spectral cutoff below 100 TeV [10]. To produce PeV particles, Ohira et al. [11] proposed a scenario of re-acceleration of particles pre-accelerated by shocks of SNRs in a pulsar wind nebula (PWN) and SNR shocks interaction system. Since most Ultra-high energy γ-ray sources are associated with PWNs, they may contribute to PeV cosmic rays significantly [12, 13].

G150.3+4.5 is a shell-type SNR. The eastern part of the shell was initially discovered by Gerbrandt et al. [14] with the faint, extended non-thermal radio emission, which was named as G150.8+3.8. Gao & Han [15] reported the total shell-like morphology with a size of $2.5^\circ \times 3.0^\circ$ using the λ6 cm survey data. The non-thermal radio spectral indices for the eastern and western shells of G150.3+4.5 are ~ -2.4 and ~ -2.7, respectively [15]. The hard power-law γ-ray emission of G150.3+4.5 was discovered by [16] by analyzing seven years of Pass 8 data recorded by the Fermi-LAT. And the γ-ray morphology is also extended with a radius of about 1.4°. Then in Fermi catalog (2FHL[17], FGES[18],4FGL [19]), G150.3+4.5, an extended source with about 1.5° is reported as a hard spectra in GeV band with index about 1.9. Devin et al. [20] use a 2D symmetric Gaussian or a disk model, spatially coincident with the radio emission, to describe the γ-ray emission detected with more than 10 years of Fermi-LAT data, and obtained a hard spectral index $\Gamma = 1.62$ at $E_0 = 9.0$ GeV with a logarithmic parabola. A unidentified source with a pulsar-like spectrum in east-southern part of the shell (above G150.8+3.8 region) was pointed out. It also geiven a possible distances of 0.3-5.0 kpc by the Hi spectrum, an unabsorbed nothermal x-ray uppler limit about 3.0×10^{-12} erg cm^{-2} s^{-1} with $\Gamma = 2.0$ and the maximum ambient density about 3.6×10^{-3} cm^{-3} estimated by ROSAT data.

2. OBSERVATIONS AND RESULTS

2.1 WCDA data Analysis and result

Using 508 days of data collected by the Water Cherenkov Detector Array (WCDA) from March 2021 to September 2022, we performed a joint likelihood fit of the spectral energy distributions (SEDs) and the extended Gaussian morphology, and the emission can be described by a power-law function(PL): $f(E) = (4.73 \pm 0.65) \times 10^{-13} (\frac{E}{3.0\text{TeV}})^{-2.66\pm0.10}$ TeV^{-1} cm^{-2} s^{-1}. The detail of fitting process can be found in Cao et al. [21]

2.2 KM2A data Analysis and result

With the data from December 2019 to September 2022, including 933 days of completed Kilometer Squared Array(KM2A) and its partial array data, we performed a joint likelihood fit of

	model	RA_{J2000} (°)	Dec_{J2000} (°)	σ(°)	TS	N_{dof}
WCDA	Extended source	67.23±0.26	55.53±0.16	1.18 ±0.12	153.8	5
KM2A	Extended source	66.63±0.11	54.63±0.05	0.32±0.06	98.0	5

Table 1: Best-fit positions and extensions with the associated statistical errors [21].The TS values and the number of degrees of freedom (N_{dof}) are given with respect to the null hypothesis (no emission from source).

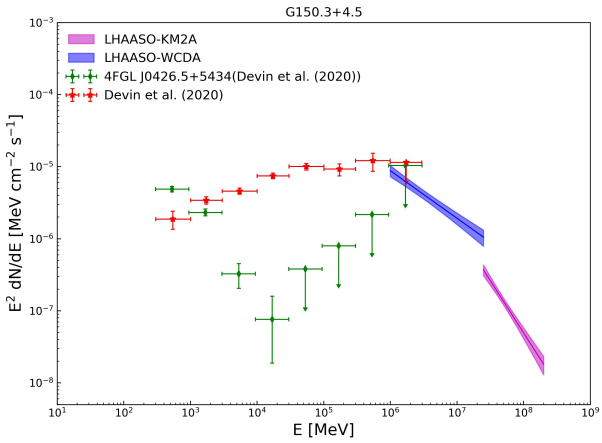

Figure 1: The gamma-ray SED of G150.3+4.5 including the Fermi-LAT data for SNR and 4FGL J0426.5+5434, and LHAASO-WCDA and LHAASO-KM2A data. The data of LHAASO from Cao et al. [21]

the spectral energy distributions (SEDs) and the extended Gaussian morphology, and the emission can be described by a power-law function(PL): $f(E) = (0.54 \pm 0.06) \times 10^{-16} (\frac{E}{50\mathrm{TeV}})^{-3.45\pm0.19}$ TeV^{-1} cm^{-2} s^{-1}. We also test the Log-Parabola function to describe the SEDs, the TS improvement of which is only 1 compared with a PL assumption, therefore, the PL is a good description of SEDs.

2.3 CO data Analysis and result

Actually, the SNR is less studied due to its large extension. Here we explored the large-scale CO emission (~20 deg^2) from the Milky Way Imaging Scroll Painting survey [i.e., the MWISP project; see details in 22] to investigate the molecular gas environment toward SNR G150.3+4.5.

Briefly, we find that the local molecular gas is probably related to SNR G150.3+4.5. The weak ^{12}CO line wings are detected for the molecular gas according to the high quality MWISP data (see details in Feng et al., in preparation). The distance of the SNR is estimated to be about less than 0.8 kpc (or the radius < 14.0 pc), leading to an an age of $\leq 1.3\times10^4$ yr for an uniform density of 1 cm^{-3}. The local density near the SNR is probably high (e.g., ~20–30 cm^{-3} for the $3.7 \times 10^4 M_\odot$ MC) and the scale height of the SNR is ≤60 pc from the Galactic plane.

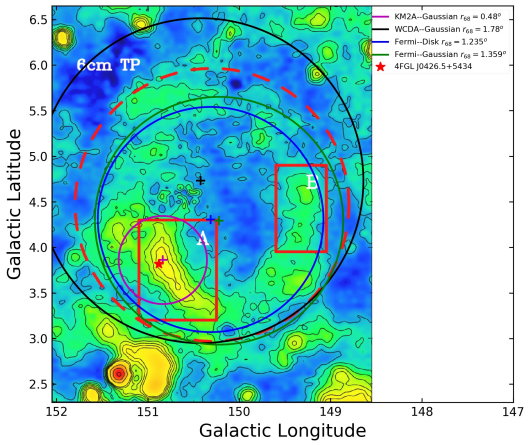

Figure 2: The morphological of radio with Urumqi 6 cm observations from Gao & Han [15].The red boxes correspond to the brightest parts of the shell. The green and blue solid lines are the best-fit models with a 2D symmetric Gaussian adn a disk model from Fermi-LAT data[20], respectively. The black and magenta solid lines represent the results of LHAASO-WCDA and LHAASO-KM2A data with a 2D-Gaussian model, respectively. The red star is a unidentified source 4FGL J0426.5+5434. The crosses are the center point of the corresponding circles.

3. Discussion

Figure 2 show the morphological of radio from Gao & Han [15], and the fitted results of Fermi-LAT [20], LHAASO-WCDA and LHAASO-KM2A [21]. We can found that the best-fit spatial models (a 2D-Gaussian: green solid line or a disk: blue solid line) of Fermi data and a 2D-Gaussian morphology (black solid line) fitted by LHAASO-WCDA data, are spatially coincident with the radio observation (red dashed line). The LHAASO-WCDA data is possible to be same origin with the radio and Fermi-LAT data. The best-fitted center point of LHAASO-KM2A data is very closed the Fermi source 4FGL J0426.5+5434, and their have the same origin. Based on the morphological of different energy band mentioned above, we propose two possible explanations for the multi-wavelength observation of SNR G150.3+4.5

3.1 Scenario: Supernova remnant plus pulsar wind nebula

Due to the morphological of radio, Fermi-LAT and LHAASO-WCDA have the same spatial structure, the radio emission and the gamma-ray from Fermi-LAT and LHAASO-WCDA come from the Supernova remnant G150.3+4.5. The unidentified source 4FGL J0426.5+5434 is considered as a pulsar. Because of the reason of the line of sight, no pulse radiation can be resolved, and the pulsar powers a pulsar wind nebula responsible for the observed GeV emission[20]. Therefore the gamma-ray from LHAASO-KM2A come from a PWN produced by accelerated electrons through IC scattering on photon fields. In Figure 2, the radio spectrum of region A is harder than that of region B [15], and the results of Gerbrandt et al. [14] imply that the radio spectral index from the region of KM2A is less than 0.38, which is agree with the spectral index of PWNe. The fitted SED of the model is showed in left panel of Figure 3. For SNR (the red lines in Figure 3)we use

the synchrotron processes and IC scattering of background soft photons with the distribution of electron, a broken power-law spectral with an super-exponential cutoff, to fit the multi-wavelength emissions. The fitting results are show: the low-end spectral index $\alpha = 2.0$, the change index $\Delta\alpha = 1.0$, the broken energy E_b^e=1.0 TeV, the cutoff energy E_c^e=50.0 TeV, the total energy content of electron above 1 GeV $W_e = 2.0 \times 10^{47}$ erg and the magnetic filed $B = 3\mu$G. For PWN (the magenta lines in Figure 3), we also use the same processes and the results are $\alpha = 1.5$, $\Delta\alpha = 1.2$, E_b^e=15.0 GeV, E_c^e=250.0 TeV, $W_e = 6.0 \times 10^{46}(\frac{D}{1.0\text{kpc}})^2$ erg and $B = 2.0\mu$G.

3.2 Scenario: Supernova remnant plus molecular cloud

The result of CO data analysis in section 2.3 show that there is an uniform density of 1 cm^{-3} and MC of higher density about $10^4 M_\odot$ for the KM2A region. Therefore the gamma-ray from KM2A region may be from high density molecular clouds interacting with high-enengy ions escaping the SNR at the early stage of the SNR evolution. The GeV emission with soft spectrum of 4FGL J0426.5+5434 is considered as to be generated by shock wave colliding with Molecular cloud. Therefore, this model consists of three parts and the result show in the right of Figure 3. One is for SNR (the red lines in Figure 3), the particles distribution trapped in SNR is described as a single power-law with an exponential cutoff, and the ratio of electron and proton is 0.01 at $E = 1$ GeV. The age of the SNR is set as the radiative energy loss time at the cutoff energy. The fitting results show: $\alpha = 1.9$, $E_c^e(B,T)$=4.0 TeV, E_c^p=60.0 TeV, $W_p = 1.5 \times 10^{49}(\frac{D}{1.0\text{kpc}})^2(\frac{n_H}{1.0\text{cm}^{-3}})^{-1}$ erg, $B = 8\mu$G and $T_{age} = 48.8$ kyr. Second is for the escaped high-energy ions (the magenta lines in Figure 3), the distribution is assumed to be proportional to

$$\frac{P^{-\alpha}}{[D(E)T]^{3/2}}\left(1-\exp\left[-\frac{\sqrt{(Pc)^2+m_p^2}}{E_{p,\text{cut}}}\right]\right)\exp\left[-\frac{R^2}{4D(E)T}-\frac{\sqrt{(Pc)^2+m_p^2}}{E_{\text{cut}}}\right],$$

where $D = D_0(E/100\text{ TeV})^{1/3}$ is the diffusion coefficient and $E_{p,\text{cut}} < E_{cut}$, R is the distance between the acceleration site and molecular cloud. The fitting results are: $E_{cut} = 0.2$ PeV, $M_{cloud} = 1.0 \times 10^4 M_\odot$ and D_0 is fixed as 4.5×10^{27} cm^2 s^{-1} [23]. we can obtained the fiting result of $R^2/4D_0T_{age} = 0.55$ with $R = 40$ pc. For comparison, we also show the result of $R = 5$ pc. Third for the shock colliding with Molecular cloud (the green lines in Figure 3). A sample single power-law with an exponential cutoff is use to fit the radio and the soft GeV emission in KM2A region. The energy cutoff of electron and proton is assumed the same. We obtain the results: $\alpha = 1.6$, $E_c^e(B,T)=E_c^p$=8.0 GeV, $W_p = 1.0 \times 10^{47}(\frac{D}{1.0\text{kpc}})^2(\frac{n_H}{160.0\text{cm}^{-3}})^{-1}$ erg, $B = 20\mu$G.

4. Conclusions

We analyzed the LHAASO-WCDA and LHAASO-KM2A data and investigated the morphological and the spectral properties of the gamma-ray from SNR G150.3+4.5. We find that a 2D-Gaussian morphology fitted by LHAASO-WCDA data is spatially coincident with the radio and Fermi-LAT observation, and the best-fitted center point of LHASSO-KM2A data is very closed the unidentified source 4FGL J0426.5+5434. The fitting results of LHAASO-WCDA and LHASSO-KM2A data all show as an extended source. We also analyzed the CO emission from the MWISP

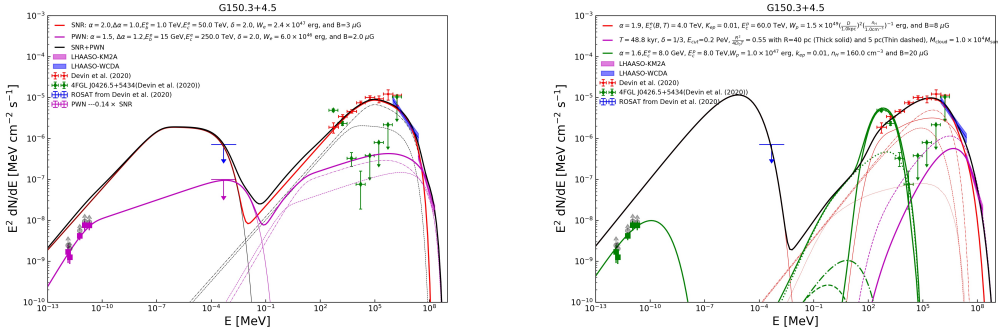

Figure 3: Left: Broadband nonthermal modeling of the SNR G150.3+4.5 for Scenario: SNR plus PWN. Right: Broadband nonthermal modeling of the SNR G150.3+4.5 for Scenario: SNR plus molecular Cloud. The radio fluxes, which are the lower limits, come from Gerbrandt et al. [14] and the radio fluxes of KM2A region is the result of the full region A minus the southern shell of region A.

project, and obtain the possible distance less than 0.8 kpc and an uniform density of 1.0 cm^{-3} with an age of $\leq 1.3\times10^4$ yr. Therefore, two scenarios are carried out to interpret the broadband nonthermal emission in region of SNR G150.3+4.5: a contribution of a supernova remnant and a PWNe or high density molecular clouds interacting with high energy proton.

Acknowledgements

The authors would like to thank all staff members who work at the LHAASO site above 4400 m above sea level year-round to maintain the detector and keep the electrical power supply and other components of the experiment operating smoothly. We are grateful to the Chengdu Management Committee of Tianfu New Area for their constant financial support of research with LHAASO data. This work is supported by the National Natural Science Foundation of China (No. 12220101003, No. 12273114, No. 12173090, No. U1931204, No. 12103040, No. 12147208 and No. U2031111), the Project for Young Scientists in Basic Research of Chinese Academy of Sciences (No. YSBR-061) and the Program for Innovative Talents and Entrepreneur in Jiangsu. This research made use of the data from the Milky Way Imaging Scroll Painting (MWISP) project. We are grateful to all the members of the MWISP working group. MWISP was sponsored by the National Key RD Program of China with grant 2017YFA0402701 and the CAS Key Research Program of Frontier Sciences with grant QYZDJ-SSW-SLH047.

References

[1] Baade, W., & Zwicky, F. 1934, Proceedings of the National Academy of Science, 20, 259, doi: 10.1073/pnas.20.5.259

[2] Drury, L. 1983, , 36, 57, doi: 10.1007/BF00171901

[3] Tavani, M., Giuliani, A., Chen, A. W., et al. 2010, , 710, L151, doi: 10.1088/2041-8205/710/2/L151

[4] Giuliani, A., Cardillo, M., Tavani, M., et al. 2011, , 742, L30, doi: 10.1088/2041-8205/742/2/L30

[5] Ackermann, M., Ajello, M., Allafort, A., et al. 2013, Science, 339, 807, doi: 10.1126/science.1231160

[6] Jogler, T., & Funk, S. 2016, , 816, 100, doi: 10.3847/0004-637X/816/2/100

[7] Tibet ASγ Collaboration, Amenomori, M., Bao, Y. W., et al. 2021, Nature Astronomy, 5, 460, doi: 10.1038/s41550-020-01294-9

[8] Albert, A., Alfaro, R., Alvarez, C., et al. 2020, , 896, L29, doi: 10.3847/2041-8213/ab96cc

[9] Zeng, H., Xin, Y., & Liu, S. 2019, , 874, 50, doi: 10.3847/1538-4357/aaf392

[10] Zeng, H., Xin, Y., Zhang, S., & Liu, S. 2021, , 910, 78, doi: 10.3847/1538-4357/abe37e

[11] Ohira, Y., Kisaka, S., & Yamazaki, R. 2018, , 478, 926, doi: 10.1093/mnras/sty1159

[12] Abeysekara, A. U., Albert, A., Alfaro, R., et al. 2020, , 124, 021102, doi: 10.1103/PhysRevLett.124.021102

[13] Cao, Zhen, F. A., An, Q., Axikegu, et al. 2021, Nature, doi: https://doi.org/10.1038/s41586-021-03498-z

[14] Gerbrandt, S., Foster, T. J., Kothes, R., Geisbüsch, J., & Tung, A. 2014, , 566, A76, doi: 10.1051/0004-6361/201423679

[15] Gao, X. Y., & Han, J. L. 2014, , 567, A59, doi: 10.1051/0004-6361/201424128

[16] Cohen, J. M. 2016, PhD thesis, University of Maryland, College Park

[17] Ackermann, M., Ajello, M., Atwood, W. B., et al. 2016, , 222, 5, doi: 10.3847/0067-0049/222/1/5

[18] Ackermann, M., Ajello, M., Baldini, L., et al. 2017, , 843, 139, doi: 10.3847/1538-4357/aa775a

[19] Abdollahi, S., Acero, F., Baldini, L., et al. 2022, , 260, 53, doi: 10.3847/1538-4365/ac6751

[20] Devin, J., Lemoine-Goumard, M., Grondin, M. H., et al. 2020, , 643, A28, doi: 10.1051/0004-6361/202038503

[21] Cao, Z., Aharonian, F., An, Q., et al. 2023, arXiv e-prints, arXiv:2305.17030, doi: 10.48550/arXiv.2305.17030

[22] Su, Y., Yang, J., Zhang, S., et al. 2019, , 240, 9, doi: 10.3847/1538-4365/aaf1c8

[23] Abeysekara, A. U., Albert, A., Alfaro, R., et al. 2017, Science, 358, 911, doi: 10.1126/science.aan4880